Granular Matter (2018) 20:56
https://doi.org/10.1007/s10035-018-0813-2

ORIGINAL PAPER

Numerical analysis of restitution coefficient, rotational speed and particle size effects on the hydrodynamics of particles in a rotating drum

Afshin Taghizadeh[1] · Seyed Hassan Hashemabadi[1] · Esmaeil Yazdani[1] · Soheil Akbari[1]

Received: 29 December 2017 / Published online: 30 July 2018

Abstract

Hydrodynamic behavior of two dimensional horizontal rotating drum was studied by using finite volume method and granular kinetic theory. In this work, the effects of the different parameters such as rotation speed, restitution coefficient and particle size on the hydrodynamic and especially on the granular temperature of particles were investigated. At first, the results of present work were verified with previous experimental results. Packing limit of 0.6 and restitution coefficient of 0.95 with Gidaspow inter-phase momentum coefficient showed the good agreement with experimental works. It is found that by increasing the restitution coefficient, the granular temperature at different depth of bed increased and affected the hydrodynamic behavior of the bed. Also, particle size and rotation speed directly changed the granular temperature. Moreover, augmentation of the rotation speed leads to increasing the repose angle which caused better mixing of bed, granular temperature rising and consequently particle velocity alteration in the bed.

Keywords Rotary bed · Granular temperature · Restitution coefficient · Computational fluid dynamics (CFD) · Particulate flow

List of symbols

C_D	Drag coefficient
d	Diameter (m)
e_{ss}	Restitution coefficient
g	Gravity acceleration (m/s^2)
g_{0ss}	Radial distribution function
$k_{\theta s}$	Energy diffusion coefficient
p	Pressure (Pascal)
p_s	Solid pressure (Pascal)
Re	Reynolds dimensionless number
t	Time
$\vec{v}$	Velocity (m/s)

Greek symbols

β	Drag coefficient between gas and solid phase
γ_s	Dissipation of the turbulent kinetic energy
ε	Volume fraction
Θ	Granular temperature
λ	Bulk viscosity
μ	Dynamic viscosity (kg/m s)
ρ	Density of gas phase (kg/m^3)
$\bar{\bar{\tau}}$	Viscous stress tensor (Pascal)
φ_s	Energy exchange between the gas and the solid phases
ω	Rotation speed (rpm)

Subscripts

col	Collisional
f	Fluid
fr	Friction
g	Gas
kin	Kinetic
max	Maximum
p	Particle
s	Solid

✉ Seyed Hassan Hashemabadi
hashemabadi@iust.ac.ir

[1] Computational Fluid Dynamics (CFD) Research Laboratory, School of Chemical Engineering, Iran University of Science and Technology (IUST), Tehran 16846-13114, Iran

1 Introduction

Many industrial processes require a large contact area between phases, which enhances heat and mass transfer. Rotating drums are usually a cylinder rotating about its central axis and provide appropriate fluid dynamics behavior for contained multiphase fluids. Rotary drums are widely used because they can process a large range of materials. Therefore, rotary drums are suitable tools to play an important role in the processing of granular materials in engineering applications as kilns, mixers, dryers and reactors. Solids motion in rotating drums is complicated. The problems of materials processing within rotary drums have been the subject of several researches lead to important information of the dynamics of granular beds, particle movements and heat transport through granular media, thus providing knowledge on how to improve the quality of products and increase production. However, the efficiency of rotary drums is highly dependent on the fluid dynamics behavior.

With increasing rotational speed of rotary drums six regimes of solid motion have been recognized as slipping, slumping, rolling, cascading, cataracting, and centrifuging [1]. In industrial cases, rolling or slumping regime is more widely used. In the rolling mode, bed material can be divided into two distinct regions, namely, a 'passive' region where particles are carried upward by the drum wall and a relatively thin 'active' region where particles flow down the sloping upper bed surface. In the passive region, the granular material moves as a rigid body and particle mixing is negligible. Particle mixing mainly occurs in the active region [2]. The rate of such a mixing determines the surface renewal rate and hence the rates of bed-freeboard heat and mass transfer, as well as chemical reactions. As a consequence, solids behavior in the active layer is extraordinarily important for the overall bed performance [2,3].

In recent years, there have been many studies that investigate the mechanics of granular flows in rotating drums. Many experimental researches have been done on this subject. Henein et al. [4] studied the effect of variables such as rotational speed, bed depth, cylinder diameter, particle size, and particle shape on bed motion in rotary kilns and batch rotary cylinders. Their experiment showed that the active-layer thickness in a rolling bed is increased with decreasing particle size and increasing rotational speed and bed depth.

Experiments on the granular flow in a rotating drum have been carried out to understand the behavior of solid particles in rotary drums. In the experiment, measurement techniques are employed to measure flow characteristics such as particle velocities and solid volume fraction. These techniques are highly expensive and time consuming. On the other hand, rotary drum concept can better observe via numerical simulations since analysis of particle behavior during rotation of drum is not easily possible, also the existing theoretical relations are not capable of considering most parameters simultaneously. Some researchers have been focused on this subject and the capability of the multiphase numerical models to predict the transverse, axial solid flow patterns and fluid flow regime. Ding et al. [2] used a 3D mathematical model to describe solids motion in the transverse plane of a rotating drum operated at low and medium rotational speeds. The modeling results showed that in rolling mode rotating drum (low to medium rotational speed) with 1.5 mm solid particles, the bed surface is flat with a dynamic repose angle of 25°. At low rotational speeds, the bed surface velocity is approximately symmetrical about the mid-chord position, but tends to be skewed with increasing rotational speed. Jarray et al. [5] investigated experimentally continuous flow in a rotating drum of dry and wet granular material. They profoundly studied the effect of capillary forces and the particle size on the flow characteristics for various rotating speeds.

Many researchers [6–10] employed frequently computational method to investigate fluid–solid motion in rotary drum, named Discrete Element Method (DEM). Their focus was on the effect of the main operating conditions (drum diameter, rotational speed and loading and particle size). DEM method describe the movement of each single particle in the bed by calculations of all interactions between the particle-particle and particle-wall and evaluating dynamic information such as transient forces acting on each particle. The main disadvantage of DEM simulations is enlarged computational complexity.

Another method used to study fluid–solid flow in a rotary bed is Euler–Euler approach. He et al. [11] and Demagh et al. [12] studied solids motion and granular viscous flow in a rotating drum using Computational Fluid Dynamics (CFD) simulations based on continuum assumption and dense phase kinetic theory in the Fluent software package. The results showed a clear two-region bed structure in the transverse plane of the drum operated in the rolling mode, an active layer with high velocity and low average concentration and a passive layer near to the drum wall with high solids concentration and low solids velocity. The velocity vectors within the active layer were not always parallel to the bed surface and at the upper limit, they make an angle of attack. They compared the numerical velocities with the experimental data, and resulted good agreement and showed that CFD model predicts well the dilute layer at the bed surface. Santos et al. [13] investigated experimentally and numerically the hydrodynamic behavior in a rotating drum under different operating conditions. The Eulerian–Eulerian multiphase model with the kinetic theory of granular flow (KTGF) was used in the simulations. They used an experimental proce-

dure to obtain directly the value of some variable related to granular flows like particle velocity. Their results indicated that the kinetic model, also can be applied in the dense granular flow to specify the rolling regime as the predicted CFD values of particle velocity were in good agreement with the experimental data. Huang et al. [14] studied solid–solid–gas three-phase motion in a rotating drum based on Eulerian continuum method coupling with kinetic theory of granular flow using CFD software Fluent. Yin et al. [15] considered a numerical simulation of 3D unsteady granular flow in rotary kiln based on the Euler–Euler two-phase flow and the kinetic theory of granular flow. Simulations showed that with increasing axial distance, the active layer thickness and velocities of granular particles increase respectively, the thickness of the active layer and velocities of particles close to the discharge end of the rotary kiln decrease. Also, the granular temperature is large in the active region where the particle exhibits fluid behavior and small in the passive region where it exhibits solid behavior, in the other words it produces in active region and transport in the passive regions. Their results depicted that particle velocity reaches its highest magnitude at the free bed surface and velocity vector of particle makes an angle with bed surface at the upper part of the active layer. Santos et al. [16] studied a hydrodynamic analysis of a rotating drum operating in the rolling regime experimentally and numerically. Also, the influence of different drag models on particle velocity profile was analyzed. For all the simulations, the Euler–Euler approach was used. Numerical results showed that the drag force can be neglected in the case of a rotating drum operated in the rolling regime where there is no fluid entering or leaving the system. On the other hand, in the active region, keeping the drum rotational speed constant, increasing the filling degree, an increase in the particle velocity magnitude occurs. In another investigation, Delele et al. [17] analyzed the solid and fluid flow behaviors inside a rotary drum using CFD model based on an Eulerian–Eulerian multiphase flow approach to study the effects of drum rotational speed, filling degree, feed rate, and drum inclination angle and found that as the rotational speed was increased, the active layer thickness and the dynamic repose angle heightened. Also, when increasing the filling degree, the surface velocity of the particle bed, the dynamic repose angle, and the active layer thickness increased.

Moreover, very little is known about the effect of restitution coefficient, particle packing limit, drum rotation speed and particle size on the bed behavior, thickness of active-passive region, velocity of solid and gas phases, and granular temperature. Thus, the purpose of this CFD study is to specify the effect of restitution coefficient, drum rotation speed and particle size on the hydrodynamic of rotating drum and especially on the particle granular temperature.

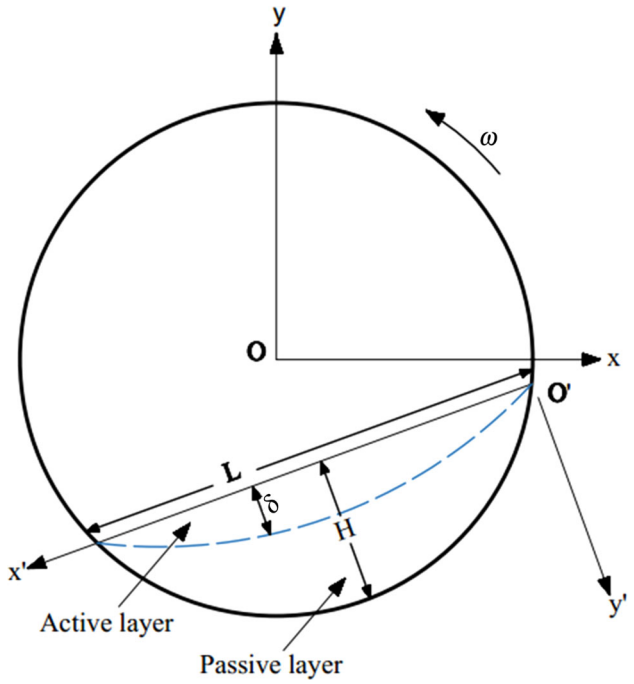

Fig. 1 Schematic of rotating drum operating on rolling regime

Table 1 Phases and simulation properties

	Description	Value
Solid phase		
$\rho_s \left(\frac{\text{kg}}{\text{m}^3}\right)$	Particle density	1164
d_p (mm)	Particle diameter	6.2
Fluid phase		
$\rho_f \left(\frac{\text{kg}}{\text{m}^3}\right)$	Fluid density	
$\mu_f \left(\frac{\text{Kg}}{\text{m}\cdot\text{s}}\right)$	Viscosity of fluid	1.8×10^{-5}
Simulation condition		
Δt (s)	Time step	1×10^{-4}
E	Relative error between iteration	1×10^{-4}
e_{ss}	Restitution coefficient	0.95
F (%)	Filling degree	18.81
$\alpha_{s.max}$	Maximum packing limit	0.6
$\omega \left(\frac{\text{rad}}{\text{s}}\right)$	Rotation speed	1.45

2 The CFD simulation model

2.1 Computational domain

Figure 1 shows the cross section of two-dimensional rotary drum that used in the present study. The drum was made of aluminum with 215 mm inner diameter. In Fig. 1 the Cartesian coordinate is located at the center of drum and assumed an apparent coordinate system that the ẋ-axis is parallel to the bed surface and the ẏ-axis is perpendicular to the bed surface,

Table 2 Governing equations

Continuity equation for gas phase	$\frac{\partial}{\partial t}\left(\varepsilon_g \rho_g\right) + \nabla.\left(\varepsilon_g \rho_g \vec{v}_g\right) = \sum_{n=1}^{N_m} R_{gs}$	(1)
Continuity equation for solid phase	$\frac{\partial}{\partial t}\left(\varepsilon_s \rho_s\right) + \nabla.\left(\varepsilon_s \rho_s \vec{v}_s\right) = \sum_{n=1}^{N_m} R_{sg}$	(2)
	$\varepsilon_g + \varepsilon_s = 1$	(3)
Momentum equation for gas phase	$\frac{\partial}{\partial t}\left(\varepsilon_g \rho_g \vec{v}_g\right) + \nabla.\left(\varepsilon_g \rho_g \vec{v}_g \vec{v}_g\right) = \varepsilon_g \nabla p + \nabla \bar{\bar{\tau}}_g + \beta_{gs}\left(\vec{v}_s - \vec{v}_g\right) + \varepsilon_g \rho_g g$	(4)
Momentum equation for solid phase	$\frac{\partial}{\partial t}\left(\varepsilon_s \rho_s \vec{v}_s\right) + \nabla.\left(\varepsilon_s \rho_s \vec{v}_s \vec{v}_s\right) = \varepsilon_s \nabla p - \nabla p_s + \nabla.\bar{\bar{\tau}}_s + \beta_{gs}\left(\vec{v}_g - \vec{v}_s\right) + \varepsilon_s \rho_s g$	(5)
Stress tensor for gas phase	$\bar{\bar{\tau}}_g = \varepsilon_g \mu_g \left\{\left[\nabla \vec{v}_g + \left(\nabla \vec{v}_g\right)^T\right] - \frac{2}{3}\nabla.\vec{v}_g \mathrm{I}\right\}$	(6)
Stress tensor for solid phase	$\bar{\bar{\tau}}_s = \varepsilon_s \mu_s \left\{\left[\nabla \vec{v}_s + \left(\nabla \vec{v}_s\right)^T\right] + \left(\varepsilon_s \lambda_s - \frac{2}{3}\varepsilon_s \mu_s\right)\nabla.\vec{v}_g \mathrm{I}\right\}$	(7)
Particulate pressure [13]	$p_s = \varepsilon_s \rho_s \Theta_s + 2\rho_s\left(1 + e_{ss}\right)\varepsilon_s^2 g_{0ss}\Theta_s$	(8)
Drag model [18]	$\begin{cases} \beta_{Ergan} = 150\frac{\varepsilon_s^2 \mu_g}{\varepsilon_g d_s^2} + 1.75\frac{\varepsilon_s \rho_g \lvert\vec{v}_s - \vec{v}_g\rvert}{d_s} & \text{for } \varepsilon_g \le 0.8 \\ \beta_{Wen-Yu} = \frac{3}{4}C_D\frac{\varepsilon_s \varepsilon_g \rho_g \lvert\vec{v}_s - \vec{v}_g\rvert}{d_s}\varepsilon_g^{-2.65} & \text{for } \varepsilon_g > 0.8 \end{cases}$	(9)
	$C_D = \begin{cases} \frac{24}{\varepsilon_g Re_s}\left[1 + 0.15\left(\varepsilon_g Re_s\right)^{0.687}\right] & \text{for } Re_s < 1000 \\ 0.44 & \text{for } Re_s \ge 1000 \end{cases}$	(10)
	$Re = \frac{\varepsilon_g \rho_g \lvert\vec{v}_s - \vec{v}_g\rvert d_s}{\mu_g}$	(11)
Kinetic theory approach		
Transport equation of granular temperature	$\frac{3}{2}\left[\frac{\partial}{\partial t}\left(\varepsilon_s \rho_s \Theta_s\right) + \nabla\left(\varepsilon_s \rho_s \Theta_s\right)\vec{v}_s\right] = \left(\nabla p_s \mathrm{I} + \varepsilon_s \nabla \bar{\bar{\tau}}_s\right) : \nabla \vec{v}_s + \nabla\left(k_{\theta s}\nabla\Theta_s\right) - \gamma_s + \varphi_s$	(12)
Dissipation of the turbulent kinetic energy [15]	$\gamma_s = 3\left(1 - e_{ss}^2\right)\varepsilon_s^2 \rho_s g_{0ss}\Theta_s\left(\frac{4}{d_p}\sqrt{\frac{\Theta_s}{\pi}} - \nabla \vec{v}_s\right)$	(13)
Radial distribution function [12]	$g_{0ss} = \left[1 - \left(\frac{\varepsilon_s}{\varepsilon_{s\max}}\right)^{1/3}\right]^{-1}$	(14)
Energy exchange between the fluid and the solid phases [19]	$\varphi_s = -3\beta_{gs}\Theta_s$	(15)
Granular shear viscosity [12,18]	$\mu_s = \mu_{s.col} + \mu_{s.kin} + \mu_{s.fr}$	(16)
	$\mu_{s.col} = \frac{4}{5}\rho_s \varepsilon_s^2 d_s g_{0ss}\left(1 + e_{ss}\right)\sqrt{\frac{\Theta_s}{\pi}}$	(17)
	$\mu_{s.kin} = \frac{10}{96}\frac{\rho_s d_s \sqrt{\Theta_s \pi}}{\left(1 + e_{ss}\right)\varepsilon_s g_{0ss}}\left(1 + \frac{4}{5}\left(1 + e_{ss}\right)\varepsilon_s g_{0ss}\right)^2$	(18)
	$\mu_{s.fr} = \frac{p_s \sin\varphi}{2\sqrt{I_{2D}}}$	(19)

to facilitate calculations. The inside of drum was meshed as a computational domain with 20,644 unstructured tetrahedral meshes.

2.2 Solid and fluid specification

The simulation parameters are assumed to be same as Santos et al. [16] study that air and soybean were considered as the gas and solid phase respectively to simulate gas–solid system (two phase flow) in the rotary drum. The fluid and solid characteristics are presented in the Table 1.

2.3 Governing equations

In the present study, a CFD model developed to predict the hydrodynamic of flow in the rotating drum. The Eulerian–Eulerian multi-phase approach, along with the kinetic theory of granular flow was used. The basic assumptions used in simulation are:

a) The particles are spherical and rigid, cohesionless and mono size.
b) The particles ensemble behaves as a continuum.
c) The granular particle bed is incompressible, and the particle density is constant.
d) Due to low Mach number (< 0.3), the gas is assumed incompressible, and the density and viscosity of the gas are constant.

Table 3 Mesh properties

Mesh number	Nodes	Skewness (maximum)	Aspect ratio range
Mesh 1	20,644	0.243	1–4.22
Mesh 2	26,405	0.213	1–2.52
Mesh 3	30,748	0.249	1–2.45

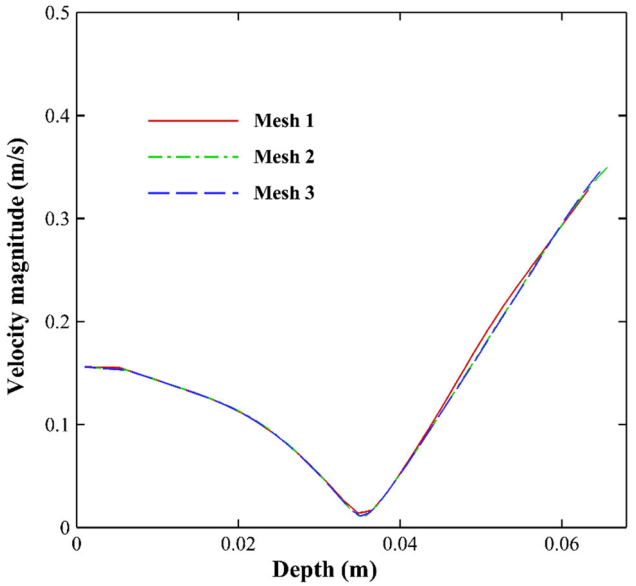

Fig. 2 Velocity magnitude of solid phase for different mesh size (1.45 rad/s rotation speed, 18.81% filling degree)

The conservation equations (mass and momentum) and other equations which were used in the simulation are presented in Table 2. Equations 1 and 2 are the mass conservation equation for gas and solid phase, respectively. The momentum equation for gas and solid phase as written as Eqs. 4 and 5. In these equations ε_g, ε_s, $\vec{v}_g$, $\vec{v}_s$, $\bar{\bar{\tau}}_g$, $\bar{\bar{\tau}}_s$, ρ_g, ρ_s, p. and p_s. are the volume fraction, velocity, viscous stress tensor, density of the gas and solid phases, fluid pressure and particulate pressure, respectively. In the present study, only drag force and gravitational force were considered on the momentum equation (β. is the drag coefficient between two phases and g. is the gravity acceleration). Equations 6 and 7 shows the Newtonian forms of viscous stress tensor for gas and solid phase, respectively, that used in momentum conservation equations. In these equations μ_g, μ_s and λ_s are the gas, solid and bulk viscosities, respectively. The particulate pressure in solid phase momentum equation is written as Eq. 8. The drag force in Eqs. 4 and 5 calculated using the model developed by Gidaspow [18] (Eqs. 9–11). Kinetic theory of granular flow was employed to calculate solid stress tensor and particulate pressure. In the kinetic theory of flow, particles move in random motion and a new term has been defined that called granular temperature, Θ., that equals to

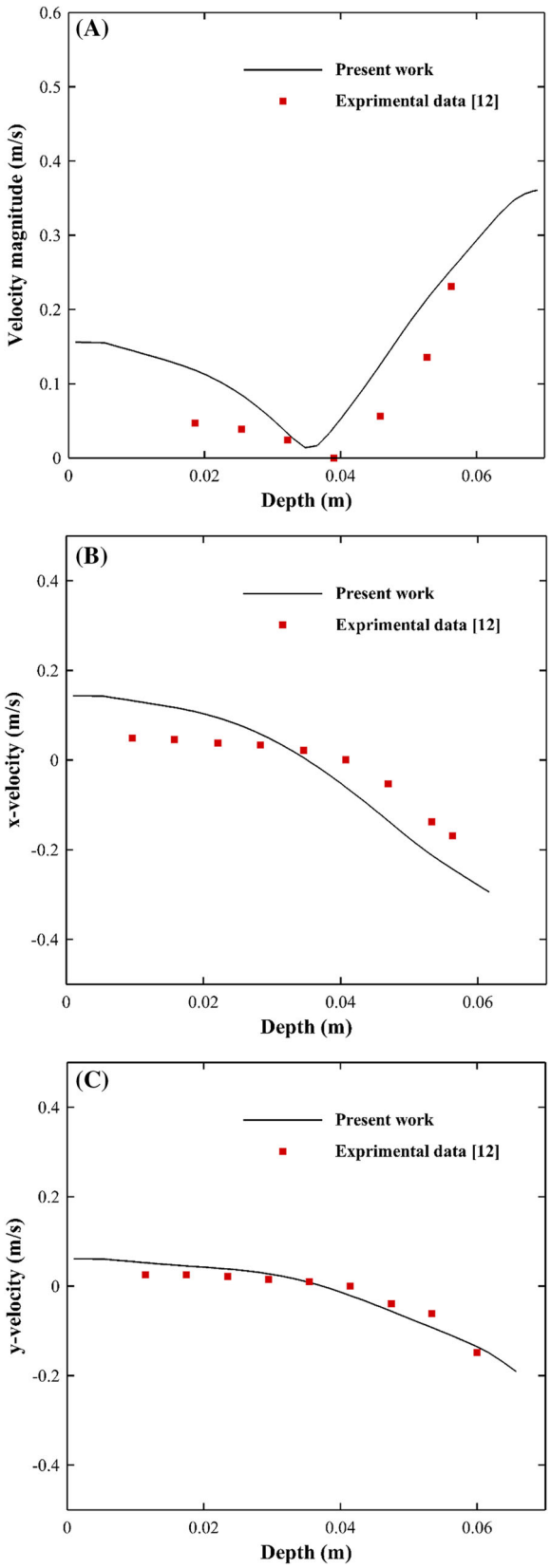

Fig. 3 Comparison of Velocity distribution of solid phase between present work and experimental data [16] (1.45 rad/s rotation speed, 18.81% filling degree); **a** velocity magnitude, **b** X-velocity, **c** Y-velocity

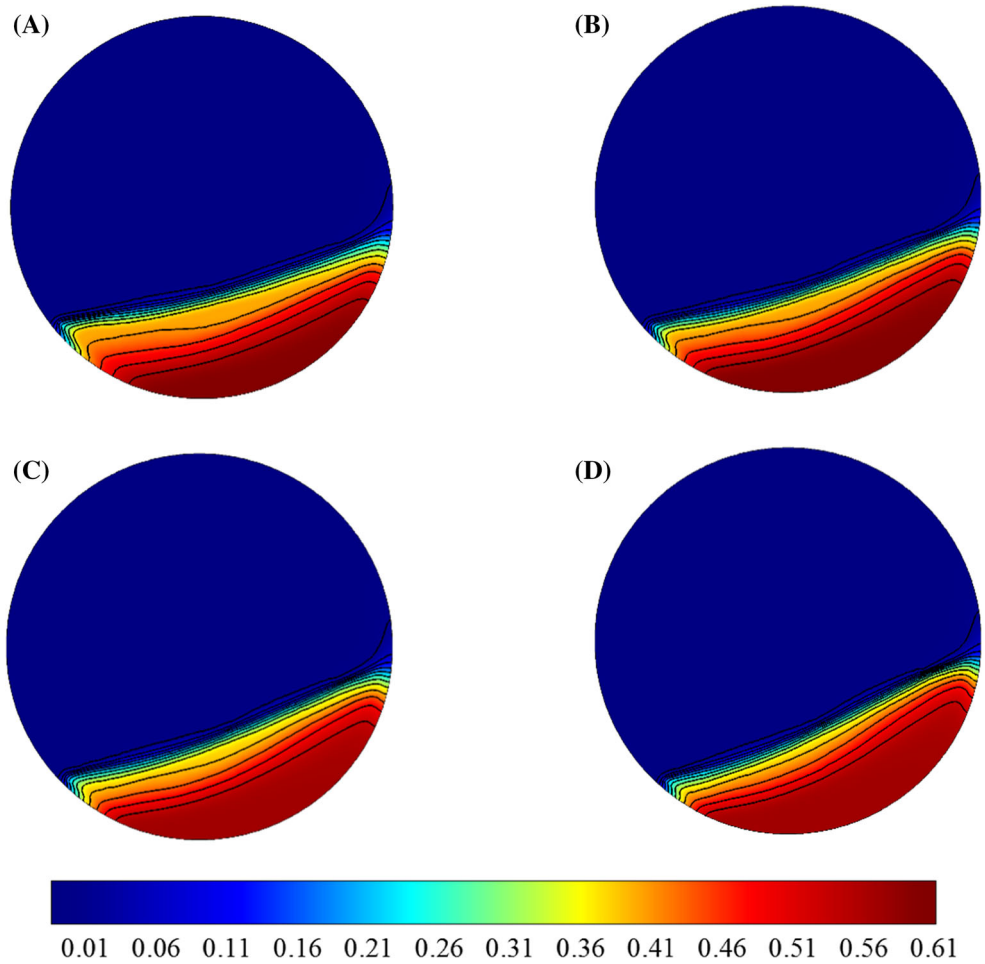

Fig. 4 Solid flow pattern and volume fraction in the rotating drum with different restitution coefficient (e_{ss}). (1.45 rad/s rotation speed, 18.81% filling degree); **a** e_{ss}: 0.95 **b** e_{ss}: 0.92 **c** e_{ss}: 0.9 **d** e_{ss}: 0.85

mean square of the random motion of particles. The granular temperature equation is written as Eq. 12. In this simulation, the algebraic rm of granular temperature transport equation was used. In this equation φ_s. and γ_s. arthe energy exchange between the fluid and the solid phases and the dissipation of the turbulent kinetic energy, respectively. g_{0ss}. is the radial distribution function that calculated by model developed by Luet al. [12]. The shear viscosity of solid phase is sum of three terms (collisional viscosity, kinetic viscosity and frictional viscosity). The Gidaspow model [18] was utilized to calculthe collisional viscosity and kinetic viscosity (Eqs. 17 and 18, respectively), and the model which is developed by Schaeffer's [12] was applied to calculate granular frictionaliscosity (Eq. 19).

2.4 Boundary conditions and numerical solution

For the drum wall, the no slip wall boundary condition was considered, with 1.45 rad/s rotation speed. At the starting of simulation, solid particles were loaded in drum, by 0.4 void fraction between particles.

In the present simulation, the equations discretized by finite volume method and the Semi Implicit Method for Pressure Linked Equation algorithm applied to simultaneous solution of governing equations [20]. In this simulation, an in-house code utilized to simulate the flow behavior in the rotating drum. All of simulations were conducted by Core i7, 2.67 GHz 8 MB cache CPU with 8 GB RAM. Other simulation conditions are presented in Table 1.

3 Results and discussion

3.1 Grid independence and validation of model

In order to study of mesh and check the independence of results from mesh characteristics, simulation performed by three tetrahedral mesh sizes. The mesh properties exist on Table 3. Figure 2 plotted the velocity magnitude along the

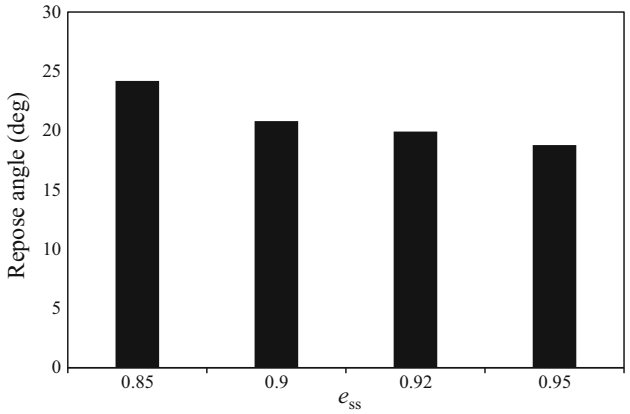

Fig. 5 The value of repose angle at different restitution coefficient (e_{ss}) (1.45 rad rotation speed, 18.81% filling degree)

perpendicular line to the bed surface for three mesh sizes. According to the Fig. 2, it can be found that three types of mesh have same result, consequently for reduction of computational cost and saving time, first mesh (mesh 1) has been chosen which has the smallest size and lowest nodes.

In order to ensure the model's accuracy, we must compare the simulation results with an experimental work, so that the model can be used in future works. Thus, the simulation results compared with Santos et al. [16] experimental data. Figure 3 shows the velocity magnitude, x-velocity and y-velocity of the simulation and the experiment. The two dimensional (2D) model simulated with conditions similar to mentioned experimental work (filling degree 18.81, rotation speed 1.54 Rad/s). As illustrated in Fig. 3, good consistency between simulation results and experimental data exists, but the negligible deviation between results may be due to either adaption or estimation of simulation parameters.

3.2 Effect of restitution coefficient on granular temperature

Before simulating solid–gas (multi-fluid) system, strain, pressure and viscosity of the solid phase should be define. For this purpose, KTGF model has been used. In this model the particles move on random motion and energy transfers by particles collisions. The fluctuation of the particle motion and energy transfer by collision cause to define a new term, which called 'granular temperature'. This parameter is equal to one third of square of solid velocity fluctuation (v_{sf}) that defines as follows:

$$\theta_s = \frac{1}{3} v_{sf}^2 \tag{20}$$

The granular temperature has significant effect on the hydrodynamic behavior of rotating drum. In this section, the effect

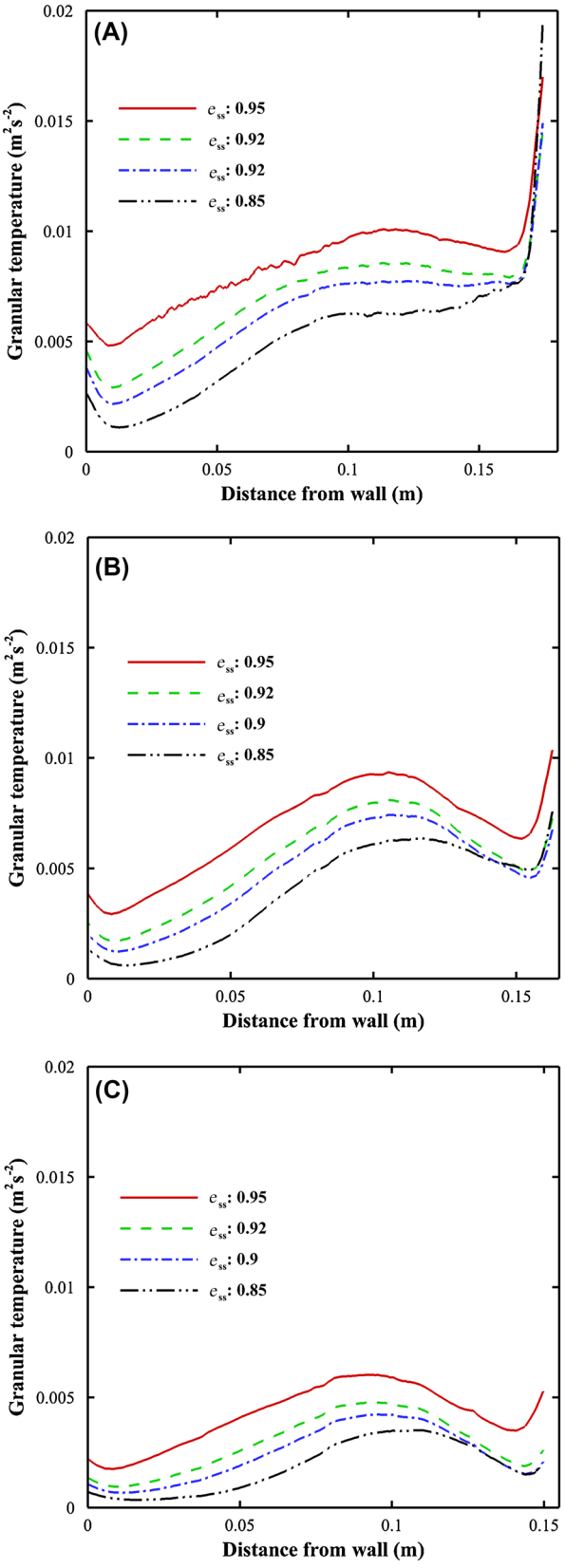

Fig. 6 Granular temperature distribution for various restitution coefficients at specific depth (ý) (1.45 rad/s rotation speed, 18.81% filling degree); **a** ý: 7 mm, **b** ý: 15 mm **c** ý: 22 mm

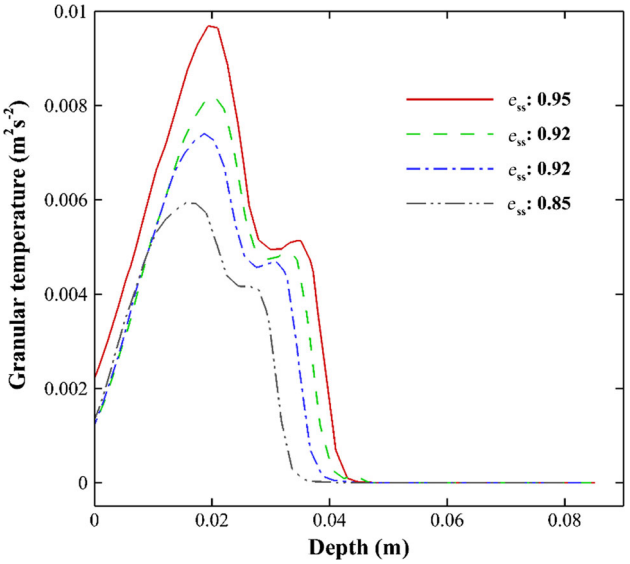

Fig. 7 Granular temperature distribution for various restitution coefficients at different depth (ý) (1.45 rad/s rotation speed, 18.81% filling degree)

of restitution coefficient (e_{ss}) on the granular temperature examined by setting the restitution coefficient to four different values (0.85, 0.9, 0.92, 0.95). The definition of restitution coefficient can be written as follows:

$$e_{ss} = \frac{\text{Speed of particle after collision}}{\text{Speed of particle before collision}} \tag{21}$$

According to the previous studies [21–23], generally, the value of restitution coefficient is not constant and depends on the impact velocity of particles, physical properties of particles and hardness ration of particles, but based on the investigation of Gorham and Kharaz [24], when the particles bed have elastic or semi-elastic behavior, can assumed a constant value for restitution coefficient . In the present study, the particle bed has semi-elastic cdition. In the CFD simulation, restitution coefficient plays role of tuning parameter, so many researchers [13,15,16,25], utilized different constant values of restitution coefficient on their simulation.

Figure 4 illustrates the solid flow pattern on the rotating drum for different restitution coefficient (e_{ss}). It can be seen that restitution coefficient has significant effect on the hydrodynamic of rotating drum and this effect was clearly identified by investigation of a repose angle. To calculate the repose angle, drawn up a line parallel to x-axis (Fig.1) and a tangent line at the bed surface, then the angle between two lines was calculated. The values of repose angle for different restitution coefficients computed and depicted in Fig. 5. According to this figure, the repose angle decreases with increasing the restitution coefficient. Thus, it can change the treatment of rotating drum on the active region.

Figure 6 shows the value of computed granular temperature on the specific bed depth for different values of restitution coefficient. The distance in the x-axis label refer to distance from the drum wall (on the apparent coordinate center side in Fig.1) at the specific bed depth.

Generally, as depicted in Fig. 6, augmentation of restitution coefficient leads to increasing the value of granular temperature. At specific bed depth near the wall boundary (such as 15 mm), the granular temperature reduced and on the central areas its value increased, demonstrated a sharp value on the diagram. This variation on the values of granular temperature can be justified that on the near wall areas the thickness of active region reduced and bed treatment will move to passive region as sooner as central region. A schematic diagram of rotating bed and active and passive region shows on Fig. 1. At thin layer sticking to the drum wall, due to no slip boundary condition, the particles move with drum wall rotation and the granular temperature suddenly increases. According to the granular temperature equation as mentioned on the Sect. 2, this parameter is proportional to solid particle velocity.

On the upper part of bed (active region), due to none zero granular temperature, the collision between particles has significant effect. High restitution coefficient indicates low dissipation of momentum at particles collision and finally resulted in enhancing the fluctuation on the solid phase, therefore the value of granular temperature increased. On the other hand, by increasing the depth, the characteristic of the solid bed moves to passive behavior. By comparison of the granular temperature on the different depths, it can be found that by increasing the depth, the value of granular temperature decline to zero. In this region, the inter-particle collisions can be negligible and the bed treats as plug flow and does not fluctuate on the particles velocity. Figure 7 shows the variation of granular temperature at different bed depth (ý). According to this figure, the point at which the granular temperature is zero, is the active/passive layer interface. On Fig. 7 it can be seen, that by increasing the restitution coefficient the active region thickness enhanced. Finally from Figs. 6 and 7, by increasing the value of restitution coefficient, active layer become thicker.

As KTGF model mentioned on the Sect. 2, the solid pressure, bulk viscosity and shear viscosity of the solid phase depend on the granular temperature values, and restitution coefficient has significant effect on granular temperature. Therefore, while simulating the hydrodynamic of the rotating drum, this parameter must be accurately determined.

3.3 Influence of rotation speed on granular temperature

By changing the rotation speed (Froude number), various regimes on the rotating drum can be observed. Six flow

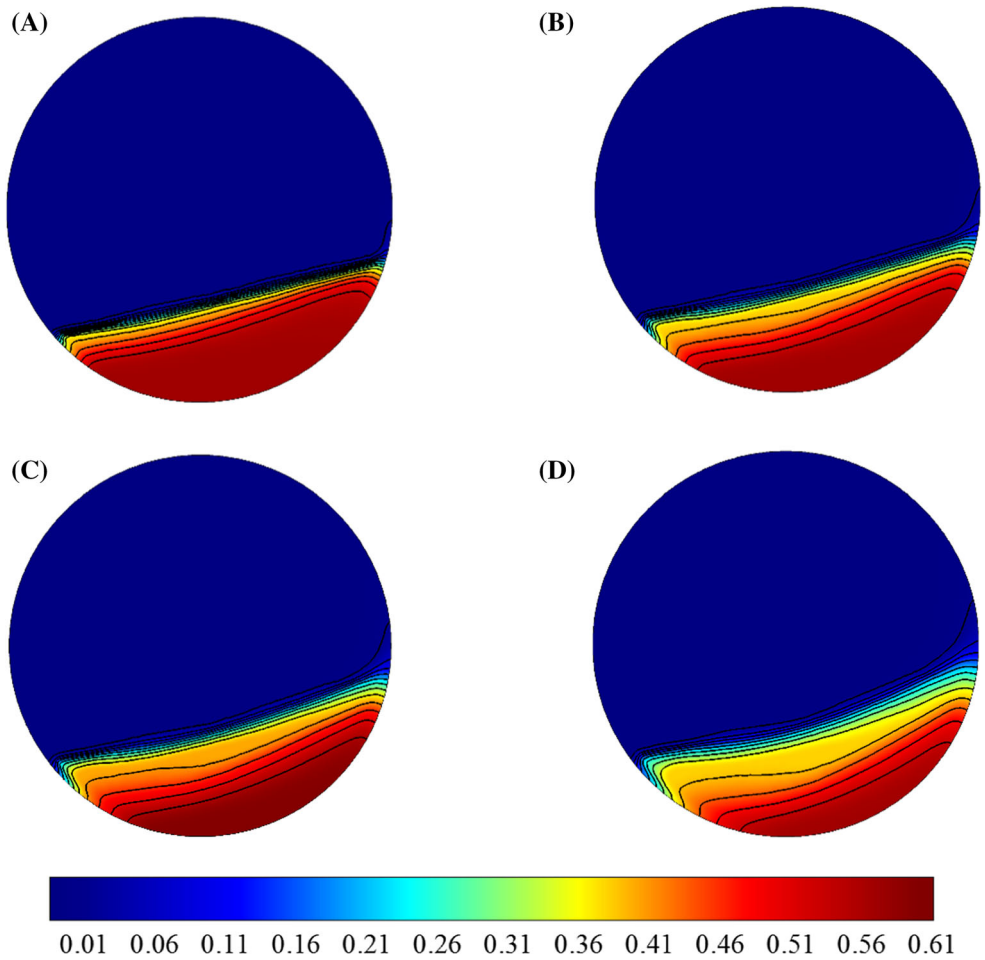

Fig. 8 Solid flow pattern and volume fraction in the rotating drum at different rotation speeds (ω) (18.81% filling degree); **a** 5 rpm **b** 10 rpm **c** 15 rpm **d** 20 rpm

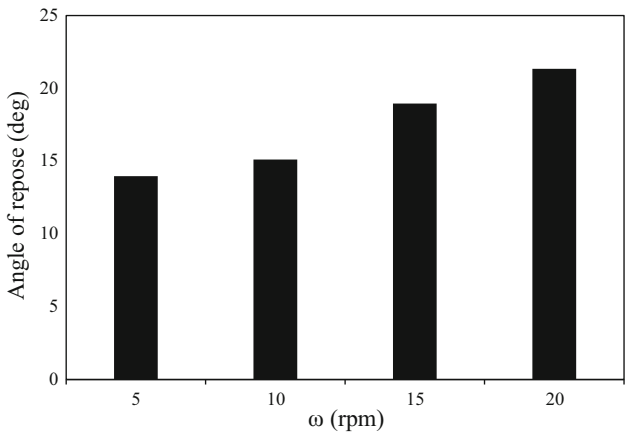

Fig. 9 The value of repose angle at different rotation speed (ω) (18.81% filling degree)

regimes on the rotating drum have been detected which classified according to increasing the rotation speed as: slipping, slumping, rolling, cascading, cataracting and centrifuging [4]. In the industrial processes, rotating drum mostly works at rolling regime. Thus, in this section rotating drum examined at different rotating speeds (5, 10, 15 and 20 rpm) on the rolling regime and effect of rotation speed on the granular temperature was investigated.

Figure 8 shows the pattern of solid phase flow on the different rotation speeds. According to the Figs. 8 and 9, it can be seen that rotation speed has significant effect on the hydrodynamic of rotating drum. By increasing the rotation speed, repose angle also increases. On the other hand, according to previous experimental studies [26–28] and numerical investigation [29], by increasing the drum rotation speed, the mean circulation time of the particle decreases and leads to improve of particles mixing in the bed.

Figure 10 shows the calculated granular temperature at specific bed depth for different rotation speeds. Reynolds number increases, by increasing the rotation speed that means to increasing the fluctuation of solid particles velocity, which according to the definition of the granular temperature in the previous section, the value of this parameter also increases as

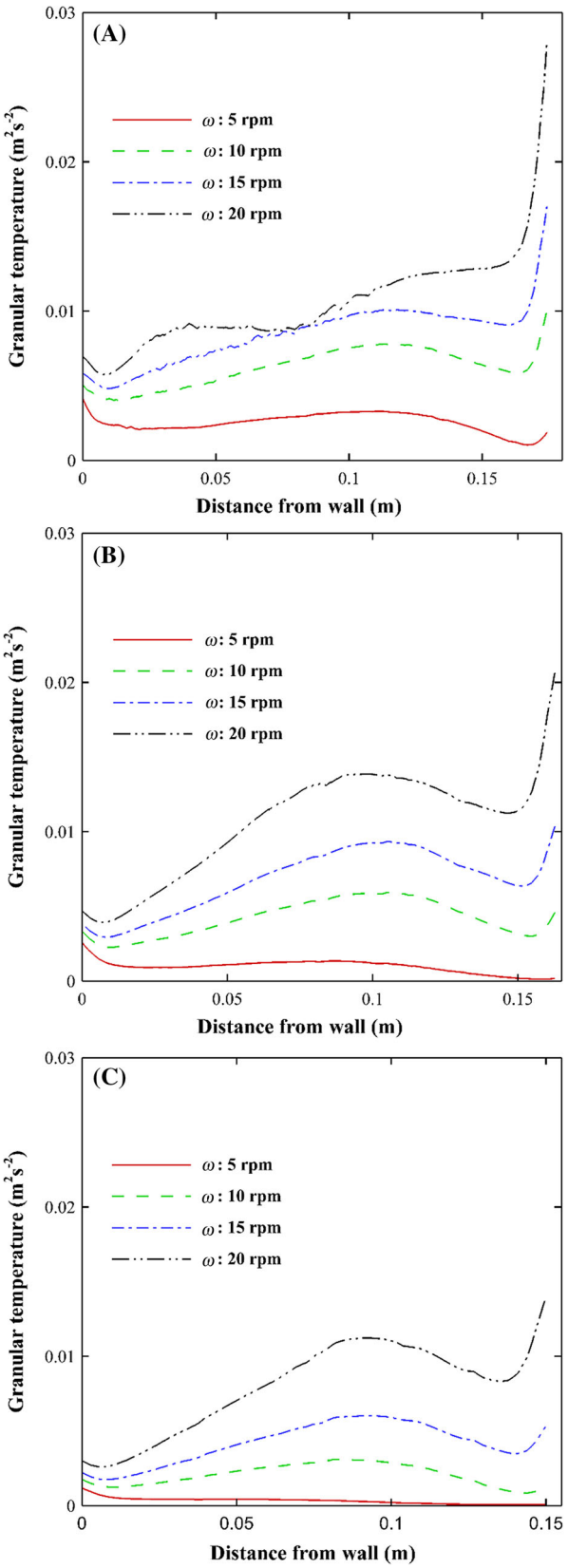

Fig. 10 Granular temperature distribution for various rotation speed (ω) at specific depth (ý) (18.81% filling degree); **a** ý: 7 mm, **b** ý: 15 mm **c** ý: 22 mm

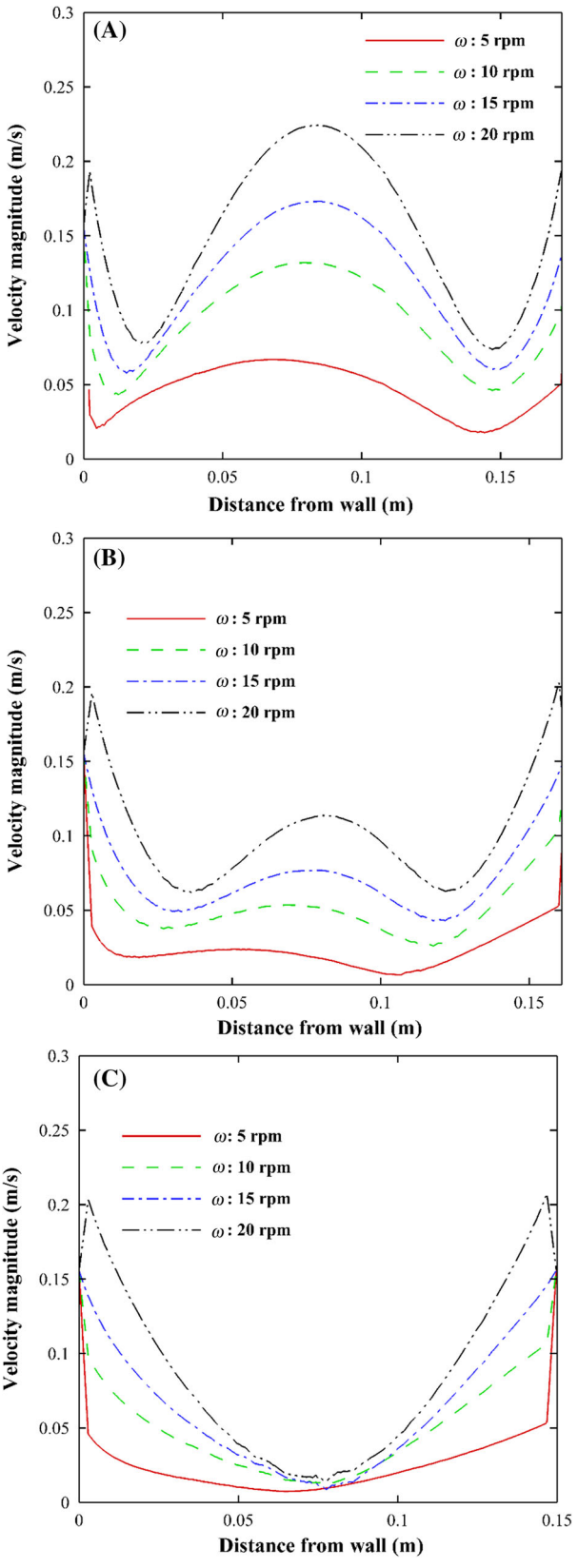

Fig. 11 Velocity magnitude distribution for various rotation speeds at specific depth (ý) (18.81% filling degree); **a** ý: 7 mm, **b** ý: 15 mm **c** ý: 22 mm

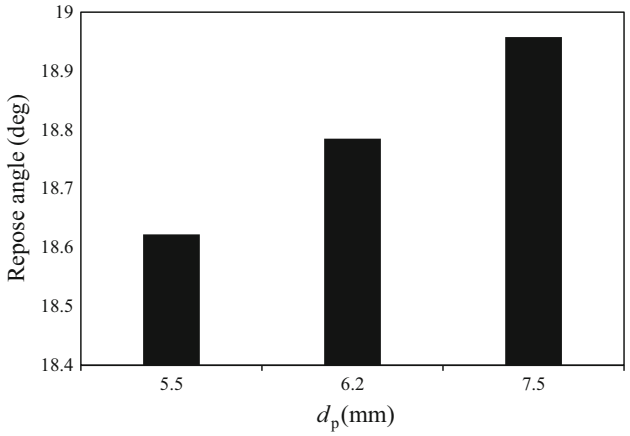

Fig. 12 The value of repose angle for different particle diameter (1.45 rad/s rotation speed, 18.81% filling degree)

shown in Fig. 10. To confirm the above mentioned description, particle velocity at specific depth for different rotation speeds depicted in Fig. 11.

According to the Fig. 10, as mentioned in previous section, by approaching to the wall the thickness of active layer reduced (lower granular temperature), but at different rotation speeds the thickness of active layer varied that it can be due to differences on repose angle value and particles bed behavior. Also, in higher rotation speeds, rising and falling of granular temperature curve is more intense.

According to the results discussed above, by setting the rotation speed at different values, different operational purpose can be obtained, but must be careful that by changing the rotation speed, the flow regime maybe alters.

3.4 Influence of particle diameter on the granular temperature

Another parameter can be effective on the granular temperature is solid particle diameter (d_p). In this section, effect of particle diameter (5.5, 6.2, 7 and 7.5 mm) on the granular temperature was studied. According to Fig. 12, it can be found that the particle diameter dose not significant effect on repose angle and it has constant value.

Figure 13 shows the computed granular temperature values at specific bed depth for different particle diameter. As illustrated in this figure, by increasing the particle diameter, granular temperature, fluctuation of particle velocity and energy transferred by collision increases. According to the equations in Sect. 2, by variation of particle diameter, turbulent kinetic energy, collisional viscosity and kinetic viscosity (Eqs. 11, 15, 16) characteristics of the solid phase will change that it causes to changing the hydrodynamic of rotating drum. On other hand, particle diameter increasing leads to heightening the Reynolds number that eventually resulted in rising the fluctuation of particles velocity on the solid phase.

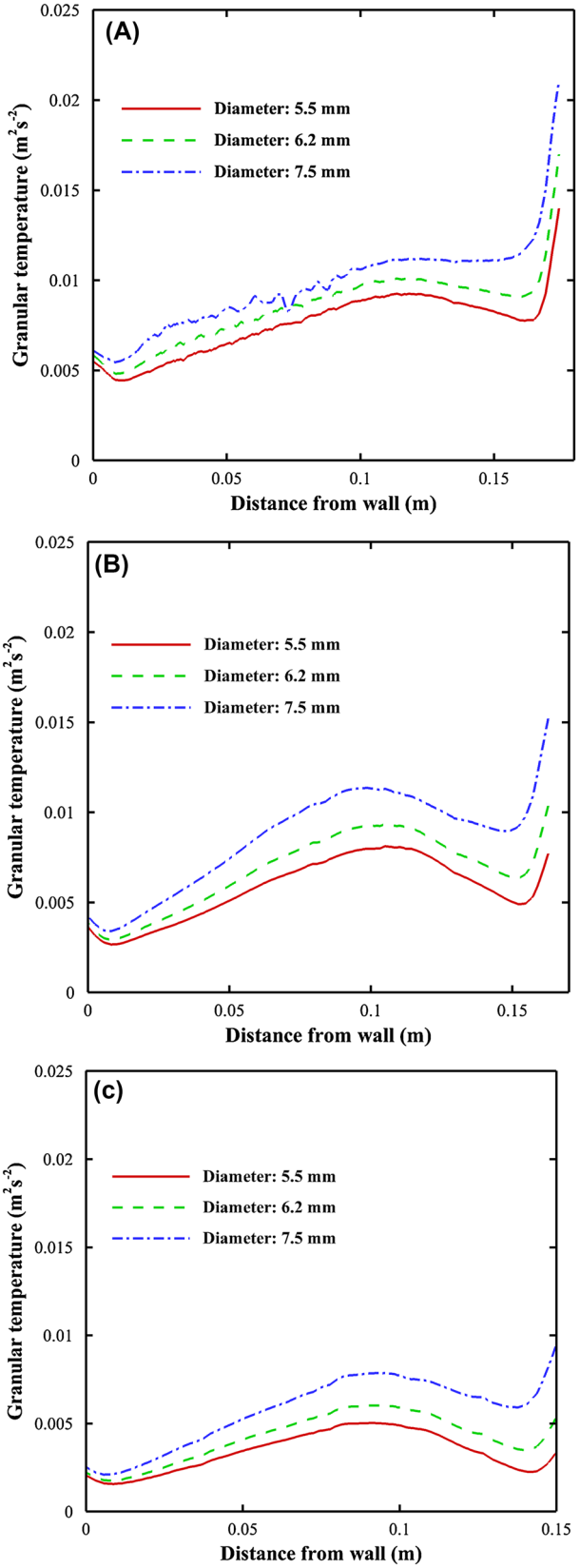

Fig. 13 Granular temperature distribution for various particle diameter at specific depth (ý) (1.45 rad/s rotation speed, 18.81% filling degree); **a** ý: 7 mm, **b** ý: 15 mm **c** ý: 22 mm

As described in previous section, while the granular temperature approaches to zero, the characteristics of solid phase flow tends to passive region behavior and it can be seen in Fig. 13 that elevation in the particle diameter leads to enhancing the granular temperature and the thickness of active layer increases.

4 Conclusion

In present study, the hydrodynamic behavior of gas–solid in the two-dimensional rotating bed was studied. In this purpose, the granular temperature was investigated by using finite volume method and granular kinetic theory. The effects of the rotation speed, coefficient of restitution and particle size on the granular temperature were studied and discussed. It was found that particle-particle restitution coefficient and rotation speed play important role in the granular temperature and consequently on the hydrodynamic behavior of the bed. In this simulation, restitution coefficients of 0.85, 0.9, 0.92 and 0.95 were investigated. When restitution coefficient is 0.95, the simulation results were close to the experimental data. Also, the effect of the rotation speeds (ω) of 5, 10, 15 and 20 rpm on the granular temperature were investigated. It was observed that with increasing the rotation speed, the granular temperature at different depth of the bed changed. Eventually, the effects of particle size were studied and resulted that by augmentation of the particle size, the granular temperature increased while it did not affect the repose angle.

Compliance with ethical standards

Conflict of interest The authors immediately certify that they have no affiliations with or involvement in any organization or entity with any financial interest or non-financial interest in the subject matter or materials discussed in this manuscript.

References

1. Mellmann, J.: The transverse motion of solids in rotating cylinders-forms of motion and transition behavior. Powder Technol. **118**, 251–270 (2001)
2. Ding, Y.L., Seville, J.P.K., Forster, R., Parker, D.J.: Solids motion in rolling mode rotating drums operated at low to medium rotational speeds. Chem. Eng. Sci. **56**, 1769–1780 (2001)
3. Dubé, O., Alizadeh, E., Chaouki, J., Bertrand, F.: Dynamics of non-spherical particles in a rotating drum. Chem. Eng. Sci. **101**, 486–502 (2013)
4. Henein, H., Brimacombe, J.K., Watkinson, A.P.: Experimental study of transverse bed motion in rotary kilns. Metall. Trans. B **14**, 191–205 (1983)
5. Jarray, A., Magnanimo, V., Luding, S.: Wet granular flow control through liquid induced cohesion. Powder Technol (2018)
6. Yang, R.Y., Yu, A.B., McElroy, L., Bao, J.: Numerical simulation of particle dynamics in different flow regimes in a rotating drum. Powder Technol. **188**, 170–177 (2008)
7. Xu, Y., Xu, C., Zhou, Z., Du, J., Hu, D.: 2D DEM simulation of particle mixing in rotating drum: a parametric study. Particuology **82**, 141–149 (2010)
8. Alizadeh, E., Bertrand, F., Chaouki, J.: Comparison of DEM results and Lagrangian experimental data for the flow and mixing of granules in a rotating drum. AIChE J. **60**, 60–75 (2014)
9. Kwapinska, M., Saage, G., Tsotsas, E.: Mixing of particles in rotary drums: a comparison of discrete element simulations with experimental results and penetration models for thermal processes. Powder Technol. **161**, 69–78 (2006)
10. Yang, S., Cahyadi, A., Wang, J., Chew, J.W.: DEM study of granular flow characteristics in the active and passive regions of a three-dimensional rotating drum. AIChE J. **62**, 3874–3888 (2016)
11. He, Y.R., Chen, H.S., Ding, Y.L., Lickiss, B.: Solids motion and segregation of binary mixtures in a rotating drum mixer. Chem. Eng. Res. Des. **85**, 963–973 (2007)
12. Demagh, Y., Ben Moussa, H., Lachi, M., Noui, S., Bordja, L.: Surface particle motions in rotating cylinders: validation and similarity for an industrial scale kiln. Powder Technol. **260**, 260–272 (2012)
13. Santos, D.A., Petri, I.J., Duarte, C.R., Barrozo, M.A.S.: Experimental and CFD study of the hydrodynamic behavior in a rotating drum. Powder Technol. **250**, 52–62 (2013)
14. Huang, A.-N., Kao, W.-C., Kuo, H.-P.: Numerical studies of particle segregation in a rotating drum based on Eulerian continuum approach. Adv. Powder Technol. **24**, 364–372 (2013)
15. Yin, H., Zhang, M., Liu, H.: Numerical simulation of three-dimensional unsteady granular flows in rotary kiln. Powder Technol. **253**, 138–145 (2014)
16. Santos, D.A., Dadalto, F.O., Scatena, R., Duarte, C.R., Barrozo, M.A.S.: A hydrodynamic analysis of a rotating drum operating in the rolling regime. Chem. Eng. Res. Des. **94**, 204–212 (2015)
17. Delele, M.A., Weigler, F., Franke, G., Mellmann, J.: Studying the solids and fluid flow behavior in rotary drums based on a multiphase CFD model. Powder Technol. **292**, 260–271 (2016)
18. Gidaspow, D.: Multiphase Flow and Fluidization: Continuum and Kinetic Theory Descriptions, 1st edn. Academic Press, Boston (1994)
19. Huilin, L., Gidaspow, D.: Hydrodynamics of binary fluidization in a riser: CFD simulation using two granular temperatures. Chem. Eng. Sci. **58**, 3777–3792 (2003)
20. Patankar, S.: Numerical Heat Transfer and Fluid Flow. CRC Press, Minnestota (1980)
21. Hussainova, I., Kübarsepp, J., Shcheglov, I.: Investigation of impact of solid particles against hardmetal and cermet targets. Tribol. Int. **32**, 337–344 (1999)
22. Labous, L., Rosato, AD., Dave, RN.: Measurements of collisional properties of spheres using high-speed video analysis. Phys. Rev. E Stat. Phys. Plasmas Fluids Relat. Interdiscip. Topics **56**, 5717–5725 (1997)
23. Ramírez, R., Pöschel, T., Brilliantov, NV., Schwager, T.: Coefficient of restitution of colliding viscoelastic spheres. Phys. Rev. E Stat. Phys. Plasmas Fluids Relat. Interdiscip. Topics **60**, 4465–4472 (1999)
24. Gorham, D.A., Kharaz, A.H.: The measurement of particle rebound characteristics. Powder Technol. **112**, 193–202 (2000)
25. Du, W., Bao, X., Xu, J., Wei, W.: Computational fluid dynamics (CFD) modeling of spouted bed: influence of frictional stress, maximum packing limit and coefficient of restitution of particles. Chem. Eng. Sci. **61**, 4558–4570 (2006)
26. Sandadi, S., Pandey, P., Turton, R.: In situ, near real-time acquisition of particle motion in rotating pan coating equipment using imaging techniques. Chem. Eng. Sci. **59**, 5807–5817 (2004)

27. Pandey, P., Turton, R.: Movement of different-shaped particles in a pan-coating device using novel video-imaging techniques. AAPS PharmSciTech **6**, E237–E244 (2005)
28. Kandela, B., Sheorey, U., Banerjee, A., Bellare, J.: Study of tablet-coating parameters for a pan coater through video imaging and Monte Carlo simulation. Powder Technol. **204**, 103–112 (2010)
29. Norouzi, H.R., Zarghami, R., Mostoufi, N.: Insights into the granular flow in rotating drums. Chem. Eng. Res. Des. **102**, 12–25 (2015)